The nonlinear elasticity of hyperelastic models for stretch-dominated cellular structures

Alexander Safar* L. Angela Mihai†

August 8, 2018

Abstract

For stretch-dominated cellular structures with arbitrarily oriented cell walls made from a homogeneous isotropic hyperelastic material, recently, continuum isotropic hyperelastic models were constructed analytically, at a mesoscopic level, from the microstructural architecture and the material properties at the cell level. Here, the nonlinear elastic properties of these models for structures with neo-Hookean cell components are derived explicitly from the strain-energy function and the finite deformation of the cell walls. First, the nonlinear shear modulus is calculated under simple shear superposed on finite uniaxial stretch. Then, the nonlinear Poisson's ratio is computed under uniaxial stretch and the nonlinear stretch modulus is obtained from a universal relation involving the shear modulus as well. The role of the nonlinear shear and stretch moduli is to quantify stiffening or softening in a material under increasing loads. Volume changes are quantified by the nonlinear bulk modulus under hydrostatic pressure. Numerical examples are presented to illustrate the behaviour of the nonlinear elastic parameters under large strains.

Key words: stretch-dominated cellular structures; isotropic hyperelastic models; nonlinear elastic parameters; multiscale large strains.

1 Introduction

Solid cellular structures are widespread in nature and in an ever increasing number of biomedical and engineering applications [10, 15, 24, 27, 28, 34, 36, 45, 51]. For example, engineered tissue scaffolds provide an environment for growth and regeneration of biological cells [9, 14, 16, 18, 19, 41, 44, 52–54], while natural materials generally incorporate several levels of structural hierarchy, which contribute to their macroscopic physical properties [22, 23, 43, 50, 55]. From the modelling point of view, a sub-level in the structural hierarchy can be treated either as a substructure with its own geometry, or as a continuum described by a suitable material model. Advancements in manufacturing techniques is also enabling the creation of new types of materials with several nested hierarchical levels [2,17,55,56]. Such structures promise to explore uncharted territory in materials research [23, 27, 50], while the recursive nature of their hierarchies brings up questions about self-similar and fractal behaviours [1, 2, 20, 31, 43].

When studying cellular structures, the common assumption is that cell walls are linearly elastic with a geometrically nonlinear behaviour. In this case, if the cell walls bend, then the elastic response can be determined from the linear-elastic deflection of a beam [27, 28]. However, in many cellular structures, when loaded, the cell walls stretch axially rather than bend. The dominant mechanical behaviour is determined by the architecture and depends on whether the cells are open or closed [11, 50]. Stretch-dominated cellular structures, such as octet-truss and body-centred cubic geometries, for example (see Figure 1), have a higher stiffness-to-weight ratio than bending-dominated ones [11, 12, 17, 23, 28, 33, 49, 50]. In addition, biological and bio-inspired materials are often nonlinearly elastic under large strains, and a finite elasticity approach is needed to understand them [29, 40, 48].

*School of Mathematics, Cardiff University, Senghennydd Road, Cardiff, CF24 4AG, UK, Email: SafarAT@cardiff.ac.uk

†School of Mathematics, Cardiff University, Senghennydd Road, Cardiff, CF24 4AG, UK, Email: MihaiLA@cardiff.ac.uk

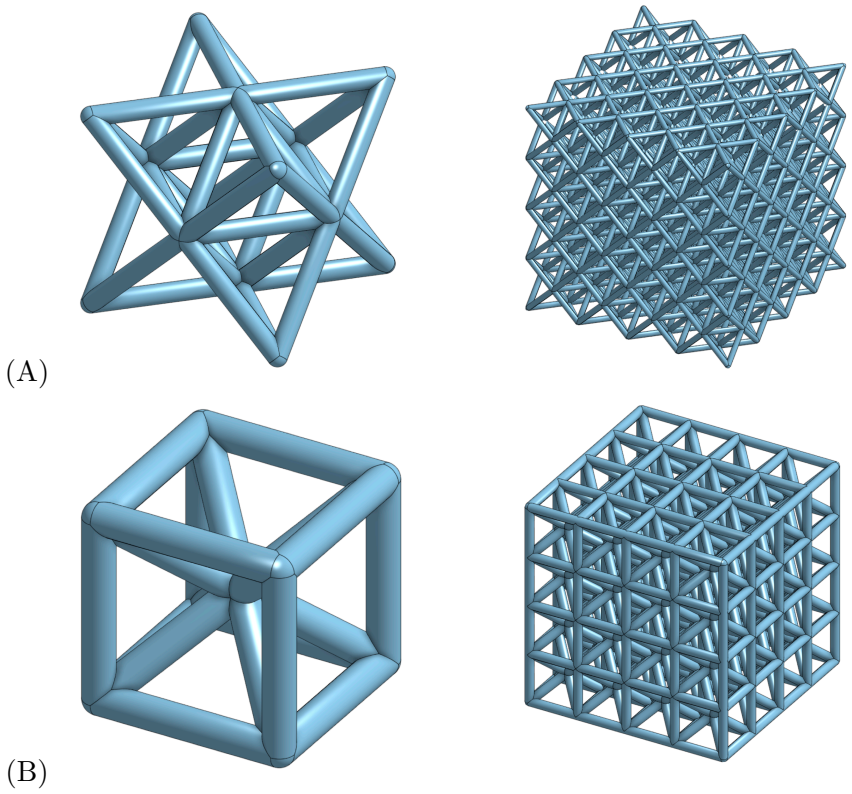

Figure 1: Examples of stretch-dominated cellular structures: (A) octet-truss and (B) body-centred cubic, at the cell level (left) and at the mesoscopic structural level (right), respectively.

Microstructure-based models for a cellular solid with open cells of isotropic linearly-elastic material were first proposed by Gent & Thomas (1959) [25], where infinitesimal stretches were assumed. In [26], these models were extended to structures with closed cells containing an ideal gas. For these models, effective Young's modulus and Poisson's ratio under infinitesimal deformations were derived explicitly from the constitutive equations [5,7]. For cellular structures of nonlinearly elastic material under finite strain deformations, a phenomenological continuum model was proposed by Blatz & Ko (1962) [8]. This model reduces to the Gent-Thomas model in the small strain limit [4,6]. Later, it was noted in [47] that Hill's energy functional of hyperelasticity [30] can be used to describe the simple special case of structures where the principal stresses are uncoupled, i.e. depend only on the stretch ratio in the corresponding principal direction. These approaches are based on Ogden-type strain-energy functions for compressible materials extending the incompressible strain-energy functions defined in [39].

For stretch-dominated structures with open or closed cells made from nonlinear elastic materials, in [37,38], novel continuum isotropic hyperelastic models, at a mesoscopic level, where the number of cells was finite and the size of the structure was comparable to the size of the cells, were constructed analytically from the structural architecture and the material properties at the cell level. For these structures, the cell walls, which were equal in size and arbitrarily oriented, were under finite triaxial deformations, while the joints between adjacent walls were not elastically deformed. The elastic responses at different scales were related by the assumption that, when the structure is subject to a triaxial stretch, each cell wall deforms also by a triaxial stretch, without bending or buckling, and the stretches of the structure and of the cell walls were related by a rotation. Possible instability effects due to cell wall buckling, for example, which could also occur under large deformations, were discussed in [37].

In this paper, we extend the theoretical investigation of the hyperelastic models for structures with neo-Hookean cell components introduced in [37, 38], by providing explicit derivations of key nonlinear elastic parameters under large strains, following the formal definition of these parameters given in [35]. In this sense, our explicit multiscale nonlinear elastic analysis and the corresponding

numerical illustrations presented here are new. First, the hyperelastic models are summarised in Section 2. Then, for each model, in Section 3, the nonlinear shear modulus is formulated explicitly under simple shear superposed on finite uniaxial stretch. In Section 4, the nonlinear Poisson's ratio is defined under uniaxial stretch and the nonlinear stretch modulus is obtained from a universal relation involving the shear modulus as well. The role of the nonlinear shear and stretch moduli is to quantify stiffening or softening in a material under increasing loads. Volume changes are quantified by the nonlinear bulk modulus under hydrostatic pressure in Section 5. The nonlinear elastic behaviour of the mesoscopic models is illustrated numerically in Section 6 and the numerical results are discussed in Section 7.

2 Hyperelastic models for stretch-dominated cellular structures

In this section, we summarise the general formulation of the continuum hyperelastic models for stretch-dominated cellular structures with open or closed cells proposed in [37,38], and specialise these models to structures with neo-Hookean cell components, which we then analyse in detail in the next sections.

2.1 Geometric assumptions

In open-cell structures, the cell walls consist of the cell edges which form an interconnected network, while in closed-cell structures, the cell walls contain both the cell edges and the cell faces forming disconnected cell compartments. For each structure, all the cell edges are equal and thin, with undeformed thickness t and length L, such that $0 < k = t/L \ll 1$, and meet at joints of approximate thickness t (see Figure 2, where the joints were slightly enlarged, emphasising that they have non-zero volume).

Open-cell structures. For the open-cell structure, we consider the case where all the cell walls are circular cylinders and the joints are spheres (see Figure 2A) [37]. Taking the unit volume as the volume of the sphere with radius $R = (L+t)/2 = L(1+k)/2$, which is centred at a joint and contains half of the length of each cell wall connected to that joint (see Figure 2B), the representative volume fraction of solid material contained in the cell walls, included in this sphere, is

$$\rho_w^{(o)} = \frac{3k^2}{(1+k)^3}. \tag{2.1}$$

Closed-cell structures. For the closed-cell structures, all the cell walls have flat faces and adjacent cell walls meet along cell edges of length L, while adjacent cell edges meet at spherical joints [38]. In this case, setting the unit volume as the volume of a sphere with radius $R = (L+t)/2 = L(1+k)/2$, centred at a joint, the representative volume fraction of solid material contained the cell walls (faces and edges) included in this sphere, is equal to

$$\rho_w^{(c)} = \frac{3k}{(1+k)^2}, \tag{2.2}$$

while the remaining volume fraction, taken by the cell core, is

$$\rho_c^{(c)} = \frac{1}{(1+k)^3}. \tag{2.3}$$

2.2 Kinematic assumptions

Stretch-dominated open-cell structures. When the structure is deformed homogeneously, with the principal stretches $\{\alpha_i\}_{i=1,2,3}$, each cell wall deforms by a triaxial stretch with the principal stretches $\{\lambda_i\}_{i=1,2,3}$. Let $(\mathbf{e}_1, \mathbf{e}_2, \mathbf{e}_3)$ be the usual orthonormal vectors for the Cartesian coordinates

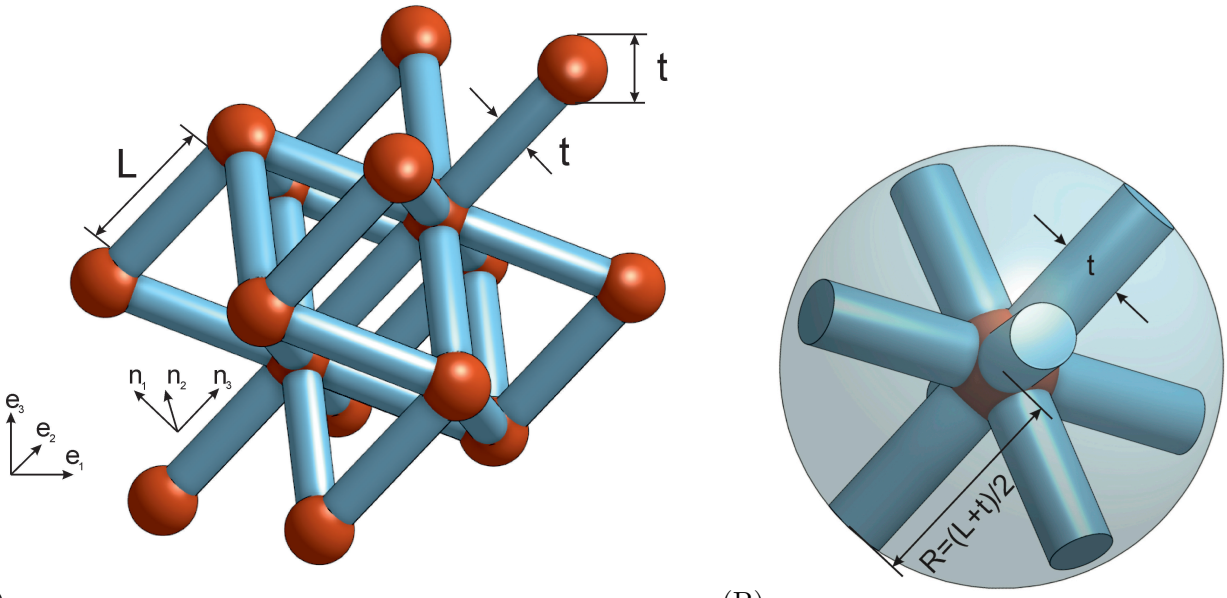

(A) (B)

Figure 2: Stretch-dominated open-cell structure: (A) geometric assumptions, and (B) unit sphere.

in the principal directions in which the structure deforms, and $(\mathbf{n}_1, \mathbf{n}_2, \mathbf{n}_3)$ denote the orthonormal vectors in the principal direction of a deforming cell wall, satisfying:

$$\begin{aligned} \mathbf{n}_1 =& -\mathbf{e}_1 \cos\theta \cos\phi - \mathbf{e}_2 \cos\theta \sin\phi + \mathbf{e}_3 \sin\theta, \\ \mathbf{n}_2 =& \mathbf{e}_1 \sin\phi - \mathbf{e}_2 \cos\phi, \\ \mathbf{n}_3 =& \mathbf{e}_1 \sin\theta \cos\phi + \mathbf{e}_2 \sin\theta \sin\phi + \mathbf{e}_3 \cos\theta. \end{aligned} \tag{2.4}$$

For the cell wall, the deformation gradient is the stretch tensor $\mathbf{F} = \mathrm{diag}(\lambda_1, \lambda_2, \lambda_3)$ and the Cauchy-Green tensor is equal to $\mathbf{C} = \mathrm{diag}(\lambda_1^2, \lambda_2^2, \lambda_3^2)$. We denote the principal invariants of the stretch tensor, $\mathbf{F}$, by

$$\begin{aligned} \iota_1 &= \lambda_1 + \lambda_2 + \lambda_3, \\ \iota_2 &= \lambda_1\lambda_2 + \lambda_2\lambda_3 + \lambda_3\lambda_1, \\ \iota_3 &= \lambda_1\lambda_2\lambda_3, \end{aligned} \tag{2.5}$$

and the principal invariants of the Cauchy-Green tensor, $\mathbf{C}$, by

$$\begin{aligned} I_1 &= \lambda_1^2 + \lambda_2^2 + \lambda_3^2, \\ I_2 &= \lambda_1^2\lambda_2^2 + \lambda_2^2\lambda_3^2 + \lambda_3^2\lambda_1^2, \\ I_3 &= \lambda_1^2\lambda_2^2\lambda_3^2. \end{aligned} \tag{2.6}$$

From (2.5) and (2.6), we obtain:

$$\begin{aligned} I_1 &= \iota_1^2 - 2\iota_2, \\ I_2 &= \iota_2^2 - 2\iota_1\iota_3, \\ I_3 &= \iota_3^2. \end{aligned} \tag{2.7}$$

Assuming that the cell joints do not deform (i.e. the elastic deformation of the joints can be neglected), if L and l are the lengths of a cell wall before and after the deformation, respectively, and t is the width of a joint between adjacent walls, we denote by $\overline{L} = L + t = (1 + k)L$ and $\overline{l} = l + t = l + kL$ the corresponding lengths of a cell element comprising a cell wall and a joint (or a cell wall and half

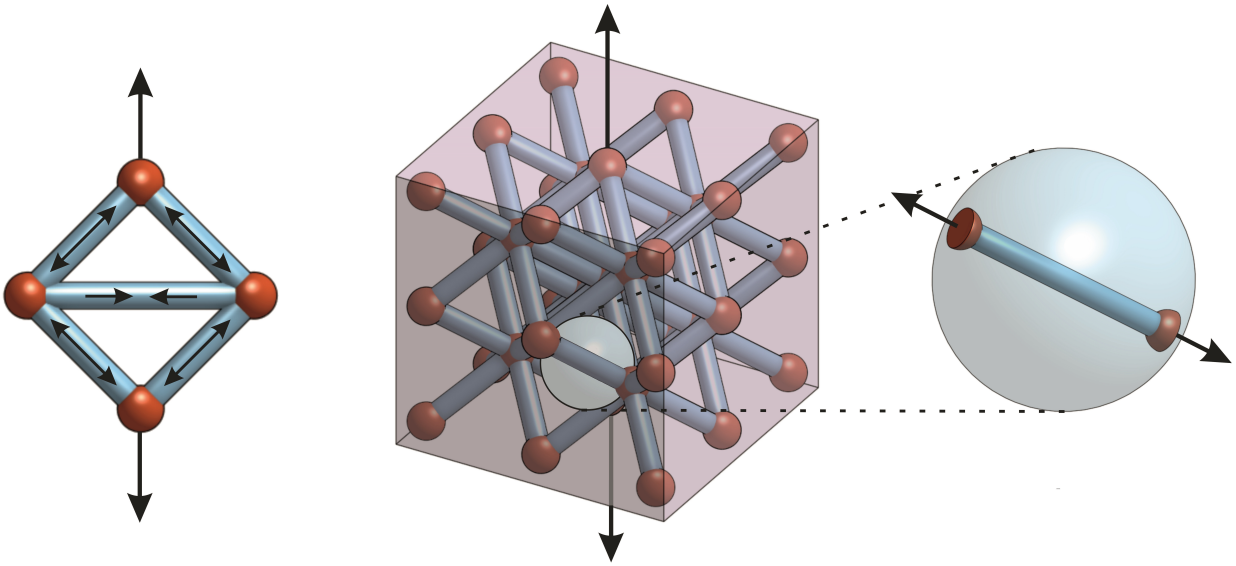

Figure 3: Stretch-dominated open-cell structure (left and middle), showing the stretching of a cell element (right).

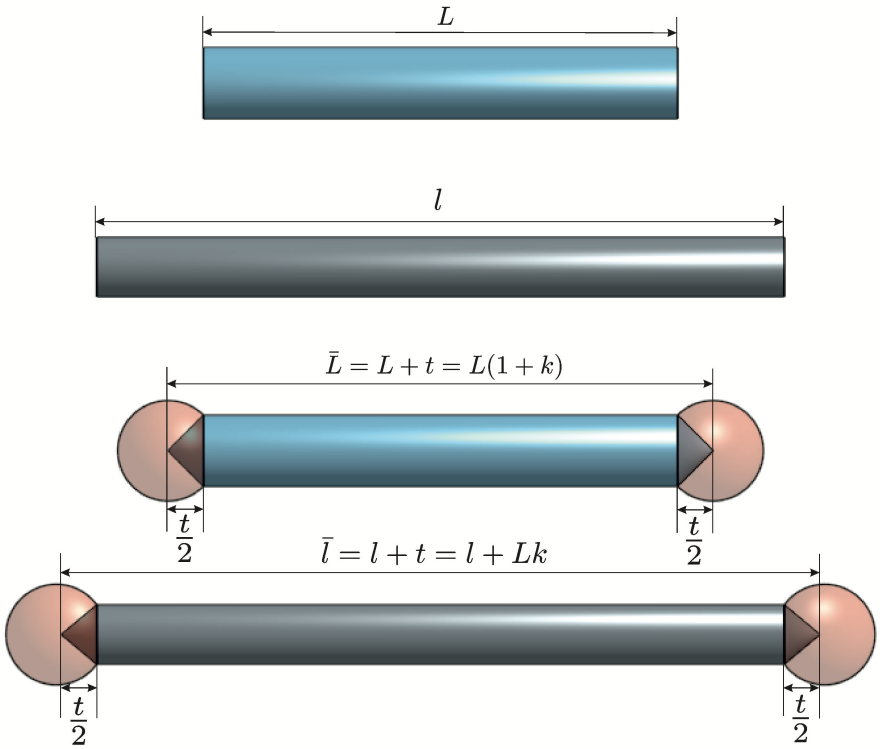

Figure 4: Cell wall and cell element before and after deformation in a stretch-dominated open-cell structure.

of each joint situated at the ends of the wall) before and after the deformation (see Figures 3 and 4). Then the principal stretches for a cell element are

$$\overline{\lambda}_i = \frac{\lambda_i + k}{1 + k}, \qquad i = 1, 2, 3, \tag{2.8}$$

and satisfy:

$$\begin{aligned}
\overline{\lambda}_1^2 =& \alpha_1^2 \cos^2\theta \cos^2\phi + \alpha_2^2 \cos^2\theta \sin^2\phi + \alpha_3^2 \sin^2\theta, \\
\overline{\lambda}_2^2 =& \alpha_1^2 \sin^2\phi + \alpha_2^2 \cos^2\phi, \\
\overline{\lambda}_3^2 =& \alpha_1^2 \sin^2\theta \cos^2\phi + \alpha_2^2 \sin^2\theta \sin^2\phi + \alpha_3^2 \cos^2\theta.
\end{aligned} \tag{2.9}$$

Denoting the principal invariants of the stretch tensor $\overline{\mathbf{F}} = \mathrm{diag}(\overline{\lambda}_1, \overline{\lambda}_2, \overline{\lambda}_3)$ by

$$\begin{aligned}
\bar{i}_1 &= \overline{\lambda}_1 + \overline{\lambda}_2 + \overline{\lambda}_3, \\
\bar{i}_2 &= \overline{\lambda}_1\overline{\lambda}_2 + \overline{\lambda}_2\overline{\lambda}_3 + \overline{\lambda}_3\overline{\lambda}_1, \\
\bar{i}_3 &= \overline{\lambda}_1\overline{\lambda}_2\overline{\lambda}_3,
\end{aligned} \tag{2.10}$$

the following relations hold between the stretch invariants (2.5) and (2.10), of the cell wall and of the cell element, respectively,

$$\begin{aligned}
\iota_1 &= (1+k)\bar{i}_1 - 3k, \\
\iota_2 &= (1+k)^2\bar{i}_2 - 2k(1+k)\bar{i}_1 + 3k^2, \\
\iota_3 &= (1+k)^3\bar{i}_3 - k(1+k)^2\bar{i}_2 + k^2(1+k)\bar{i}_1 - k^3.
\end{aligned} \tag{2.11}$$

Then, by (2.7) and (2.11),

$$\begin{aligned}
I_1 &= \left[(1+k)\bar{i}_1 - 3k\right]^2 - 2\left[(1+k)^2\bar{i}_2 - 2k(1+k)\bar{i}_1 + 3k^2\right] \\
I_2 &= \left[(1+k)^2\bar{i}_2 - 2k(1+k)\bar{i}_1 + 3k^2\right]^2 \\
&\quad - 2\left[(1+k)\bar{i}_1 - 3k\right]\left[(1+k)^3\bar{i}_3 - k(1+k)^2\bar{i}_2 + k^2(1+k)\bar{i}_1 - k^3\right], \\
I_3 &= \left[(1+k)^3\bar{i}_3 - k(1+k)^2\bar{i}_2 + k^2(1+k)\bar{i}_1 - k^3\right]^2.
\end{aligned} \tag{2.12}$$

For the structure, the principal invariants of the stretch tensor are:

$$\begin{aligned}
i_1 &= \alpha_1 + \alpha_2 + \alpha_3, \\
i_2 &= \alpha_1\alpha_2 + \alpha_2\alpha_3 + \alpha_3\alpha_1, \\
i_3 &= \alpha_1\alpha_2\alpha_3.
\end{aligned} \tag{2.13}$$

Stretch-dominated closed-cell structures. For the closed-cell structures, the kinematic assumptions on the cell walls and the cell joints are the same as for the open-cell case. In addition, when the cells are filled with an isotropic hyperelastic core, it is assumed that the cell core is in full active contact with the adjacent cell walls throughout the deformation, i.e. there are no gaps between the walls and the core in a deforming cell.

Remark 2.1 *We note that, in order for the kinematic assumptions to be satisfied, and in particular, that the deformation of the cell walls can be approximated by a triaxial stretch, while the elastic deformation of the joints may be neglected, it is reasonable to assume that the thickness of the walls, t, is much smaller than the length of the walls, L, and hence $k = t/L$ is sufficiently small, i.e. $0 < k \ll 1$. In practice, the upper limit for k, such that the kinematic assumptions are reasonably satisfied, will depend on both the cell wall material and cell geometry. In particular, under the geometric and kinematic assumptions decribed above, in [37], numerical examples show that the mesoscopic models capture the behaviour of cellular structures with a fixed number of cells and increasing wall thickness more accurately for the structures with thinner walls, where the deformation of the walls is closer to the triaxial stretch and the joints deform less significantly, as assumed theoretically, than for those with thicker walls, where the theoretical assumptions fail to be satisfied. In the numerical examples presented in Section 6 of this paper, we compare numerically the nonlinear material properties of the mesoscopic models, by taking $k \in \{0.1, 0.2, 0.3\}$ and the cell wall material parameters fixed, or varying the cell core material parameters while the cell wall material and $k = 0.1$ are fixed.*

2.3 Constitutive models

First, we recall that, for a homogeneous isotropic hyperelastic material, the following principles hold:

- Material objectivity (frame indifference), which states that the constitutive equation must be invariant under changes of frame of reference, i.e. the scalar strain-energy function, $W = W(\mathbf{F})$, depending only on the deformation gradient $\mathbf{F}$, with respect to the reference configuration, is unaffected by a superimposed rigid-body transformation (which involves a change of position) after deformation, i.e. $W(\mathbf{R}^T\mathbf{F}) = W(\mathbf{F})$, where $\mathbf{R} \in SO(3)$ is a proper orthogonal tensor (rotation).

- Material isotropy, which requires that the strain-energy function is unaffected by a superimposed rigid-body transformation prior to deformation, i.e. $W(\mathbf{FQ}) = W(\mathbf{F})$, where $\mathbf{Q} \in SO(3)$.

Then, assuming that the cell walls are made from a homogeneous isotropic hyperelastic material, by (2.9), (2.12), and (2.13), the strain-energy function of the cell walls takes the equivalent forms

$$\mathcal{W}_w(I_1, I_2, I_3) = \overline{\mathcal{W}}_w(\bar{i}_1, \bar{i}_2, \bar{i}_3) = \overline{\mathcal{W}}_w(i_1, i_2, i_3). \tag{2.14}$$

Open-cell model. For the open-cell mesoscopic model, the strain-energy function per unit volume is defined by taking the mean value of the cell wall energy over the unit sphere [37],

$$\begin{aligned} \mathcal{W}^{(o)}(i_1, i_2, i_3) &= \rho_w^{(o)} \frac{2}{\pi} \int_0^{\pi/2} \int_0^{\pi/2} \overline{\mathcal{W}}_w(i_1, i_2, i_3) \sin\theta \mathrm{d}\theta \mathrm{d}\phi \\ &= \rho_w^{(o)} \overline{\mathcal{W}}_w(i_1, i_2, i_3). \end{aligned} \tag{2.15}$$

The principal components of the corresponding Cauchy stress tensor are

$$\begin{aligned} \sigma_i^{(o)} &= J_o^{-1} \alpha_i \frac{\partial \mathcal{W}^{(o)}}{\partial \alpha_i} \\ &= J_o^{-1} \frac{\partial \mathcal{W}^{(o)}}{\partial (\ln \alpha_i)}, \qquad i = 1, 2, 3, \end{aligned} \tag{2.16}$$

where $J_o = i_3 = \alpha_1\alpha_2\alpha_3$.

Closed-cell model. For the closed-cell mesoscopic model, the strain-energy function is equal to [38]

$$\mathcal{W}^{(c)}(i_1, i_2, i_3) = \rho_w^{(c)} \overline{\mathcal{W}}_w(i_1, i_2, i_3) + \rho_c^{(c)} \mathcal{W}_c(i_1, i_2, i_3), \tag{2.17}$$

where $\overline{\mathcal{W}}_w(i_1, i_2, i_3)$ and $\mathcal{W}_c(i_1, i_2, i_3)$ are the strain-energy functions for the cell walls and the cell core, respectively. When the cells are empty, the hyperelastic model defined by (2.17) simplifies to

$$\mathcal{W}^{(e)}(i_1, i_2, i_3) = \rho_w^{(c)} \overline{\mathcal{W}}_w(i_1, i_2, i_3). \tag{2.18}$$

The principal components of the associated Cauchy stress tensor are

$$\begin{aligned} \sigma_i^{(c)} &= J_c^{-1} \alpha_i \frac{\partial \mathcal{W}^{(c)}}{\partial \alpha_i} \\ &= J_c^{-1} \frac{\partial \mathcal{W}^{(c)}}{\partial (\ln \alpha_i)}, \qquad i = 1, 2, 3, \end{aligned} \tag{2.19}$$

where $J_c = i_3 = \alpha_1\alpha_2\alpha_3$.

2.4 Hierarchical and self-similar structures

As the strain-energy functions for the isotropic hyperelastic cell wall and cell core materials can be chosen arbitrarily, the mesoscopic models for open- or closed-cell structures given by (2.15) and (2.17), respectively, can be applied iteratively to create hierarchical or self-similar structures. In this case, the cell walls would consist of stretch-dominated architectures with open or closed cells. For a model to be classified as self-similar, the geometric and kinematic assumptions must hold on multiple levels.

2.5 The particular case with neo-Hookean cell components

To investigate the nonlinear elastic behaviour of the constitutive models (2.15) and (2.17), we specialise to the case where the cell wall material is described by the neo-Hookean model

$$\mathcal{W}_w(I_1,I_2,I_3)=\frac{\mu_w}{2}\left(I_1-3-\ln I_3\right)+\frac{\lambda_w}{2}\left(\ln I_3^{1/2}\right)^2, \tag{2.20}$$

with μ_w and λ_w positive constants.

Open cells with neo-Hookean cell walls. The strain-energy function for the open-cell model (2.15) with the cell wall material described by (2.20) is equal to [37]

$$\begin{aligned}\mathcal{W}^{(o)}(i_1,i_2,i_3)=&\frac{\mu_w\rho_w^{(o)}}{2}\left[(1+k)^2\left(i_1^2-2i_2\right)-2k(1+k)i_1-3\left(1-k^2\right)\right]\\&-\mu_w\rho_w^{(o)}\ln\left[(1+k)^3i_3-k(1+k)^2i_2+k^2(1+k)i_1-k^3\right]\\&+\frac{\lambda_w\rho_w^{(o)}}{2}\left\{\ln\left[(1+k)^3i_3-k(1+k)^2i_2+k^2(1+k)i_1-k^3\right]\right\}^2.\end{aligned} \tag{2.21}$$

The associated principal Cauchy stress components, given by (2.16), are

$$\begin{aligned}\sigma_i^{(o)}=&\mu_w\rho_w^{(o)}(1+k)\frac{\alpha_i}{\alpha_1\alpha_2\alpha_3}\left[\alpha_i(1+k)-k-\frac{1}{\alpha_i(1+k)-k}\right]\\&+\lambda_w\rho_w^{(o)}(1+k)\frac{\alpha_i}{\alpha_1\alpha_2\alpha_3}\frac{\ln\left[(1+k)^3i_3-k(1+k)^2i_2+k^2(1+k)i_1-k^3\right]}{\alpha_i(1+k)-k},\qquad i=1,2,3.\end{aligned} \tag{2.22}$$

Closed cells with neo-Hookean components. For the closed-cell structures, if the cells are filled, we also assume that the cell core is characterised by the neo-Hookean model

$$\mathcal{W}_c(I_1,I_2,I_3)=\frac{\mu_c}{2}\left(I_1-3-\ln I_3\right)+\frac{\lambda_c}{2}\left(\ln I_3^{1/2}\right)^2, \tag{2.23}$$

with μ_c, λ_c positive constants. Then, the strain-energy function for the closed-cell model (2.17) takes the form [38]

$$\begin{aligned}\mathcal{W}^{(c)}(i_1,i_2,i_3)=&\frac{\mu_w\rho_w^{(c)}}{2}\left[(1+k)^2\left(i_1^2-2i_2\right)-2k(1+k)i_1-3\left(1-k^2\right)\right]\\&-\mu_w\rho_w^{(c)}\ln\left[(1+k)^3i_3-k(1+k)^2i_2+k^2(1+k)i_1-k^3\right]\\&+\frac{\lambda_w\rho_w^{(c)}}{2}\left\{\ln\left[(1+k)^3i_3-k(1+k)^2i_2+k^2(1+k)i_1-k^3\right]\right\}^2\\&+\rho_c^{(c)}\left[\frac{\mu_c}{2}\left(i_1^2-2i_2-3-2\ln i_3\right)+\frac{\lambda_c}{2}\left(\ln i_3\right)^2\right].\end{aligned} \tag{2.24}$$

The associated principal Cauchy stresses, given by (2.19), are

$$\begin{aligned}\sigma_i^{(c)}=&\mu_w\rho_w^{(c)}(1+k)\frac{\alpha_i}{\alpha_1\alpha_2\alpha_3}\left[\alpha_i(1+k)-k-\frac{1}{\alpha_i(1+k)-k}\right]\\&+\lambda_w\rho_w^{(c)}(1+k)\frac{\alpha_i}{\alpha_1\alpha_2\alpha_3}\frac{\ln\left[(1+k)^3i_3-k(1+k)^2i_2+k^2(1+k)i_1-k^3\right]}{\alpha_i(1+k)-k}\\&+\frac{\rho_c^{(c)}}{\alpha_1\alpha_2\alpha_3}\left[\mu_c\left(\alpha_i^2-1\right)+\lambda_c\ln i_3\right],\qquad i=1,2,3.\end{aligned} \tag{2.25}$$

3 Shear modulus

In this section, we provide explicit derivations of the nonlinear shear moduli for the mesoscopic models (2.21) and (2.24) under large strains, following the formal definitions given in [35]. For the values of these parameters under infinitesimal deformations, we refer also to [37] and [38]. We consider the following multiaxial homogeneous deformation [21,46], consisting of simple shear superposed on finite uniaxial stretch (see Figure 5) [13,35,42],

$$\begin{aligned} x_1 &= \alpha(a)X_1 + \gamma a X_3, \\ x_2 &= \alpha(a)X_2, \\ x_3 &= aX_3, \end{aligned} \tag{3.1}$$

where (X_1, X_2, X_3) and (x_1, x_2, x_3) are the Cartesian coordinates for the Lagrangian (reference) and the Eulerian (current) configuration, respectively, and a and γ are positive constants.

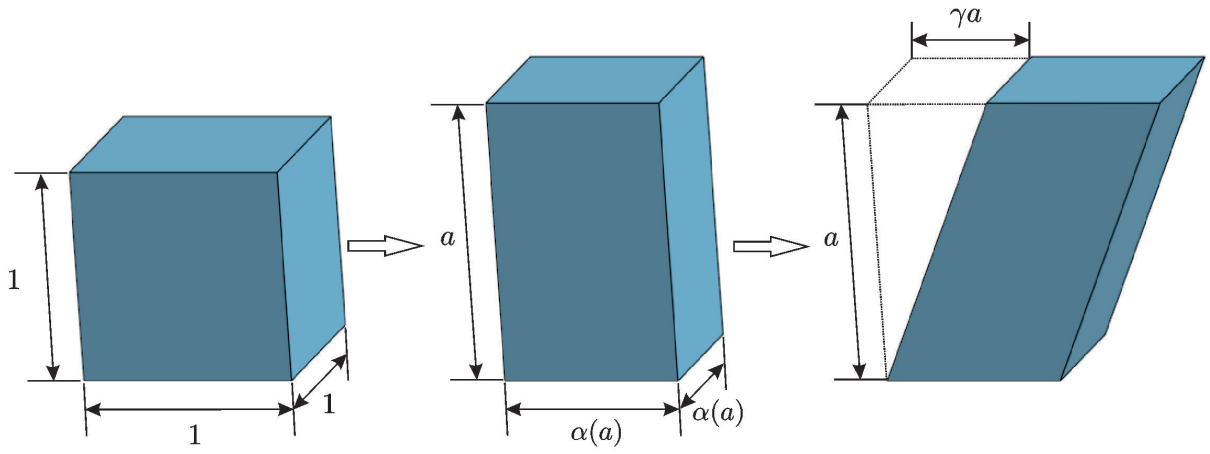

Figure 5: Cuboid (left) deformed by uniaxial stretch (middle) followed by simple shear (right).

For this deformation, the principal stretches $\{\alpha_i\}_{i=1,2,3}$ satisfy

$$\begin{aligned} \alpha_1^2 &= \frac{\alpha(a)^2 + a^2\left(1+\gamma^2\right) + \sqrt{\left[\alpha(a)^2 + a^2\left(1+\gamma^2\right)\right]^2 - 4a^2\alpha(a)^2}}{2}, \\ \alpha_2^2 &= \frac{\alpha(a)^2 + a^2\left(1+\gamma^2\right) - \sqrt{\left[\alpha(a)^2 + a^2\left(1+\gamma^2\right)\right]^2 - 4a^2\alpha(a)^2}}{2}, \\ \alpha_3^2 &= \alpha(a)^2. \end{aligned} \tag{3.2}$$

Then, $J = \alpha_1\alpha_2\alpha_3 = a\alpha(a)^2$.

For both compressible and incompressible materials, a *nonlinear shear modulus* is defined in [35] as

$$\mu(a,\gamma) = \frac{\sigma_1 - \sigma_2}{\alpha_1^2 - \alpha_2^2}, \tag{3.3}$$

where $\{\sigma_i\}_{i=1,2,3}$ are the principal components of the Cauchy stress tensor associated with the deformation (3.1).

Remark 3.1 *Note that the nonlinear shear modulus given by* (3.3) *is positive if the Baker-Ericksen (BE) inequalities hold. These inequalities state that the greater principal Cauchy stress occurs in the direction of the greater principal stretch, i.e.*

$$(\sigma_i - \sigma_j)(\alpha_i - \alpha_j) > 0 \quad \textit{if} \quad \alpha_i \neq \alpha_j, \quad i,j = 1,2,3, \tag{3.4}$$

with "$\geq$" replacing the strict inequality "$>$" if any two principal stretches are equal [3, 32].

When $a \to 1$, i.e. for simple shear superposed on infinitesimal axial stretch, the nonlinear shear modulus given by (3.3) converges to the nonlinear shear modulus for simple shear,

$$\widehat{\mu}(\gamma) = \lim_{a\to 1} \mu(a,\gamma), \tag{3.5}$$

and the principal stretches satisfy

$$\begin{aligned}
\widehat{\alpha}_1^2 &= 1 + \frac{\gamma^2 + \gamma\sqrt{\gamma^2+4}}{2} = \alpha^2,\\
\widehat{\alpha}_2^2 &= 1 + \frac{\gamma^2 - \gamma\sqrt{\gamma^2+4}}{2} = \alpha^{-2},\\
\widehat{\alpha}_3^2 &= 1.
\end{aligned}$$

Similarly, when $\gamma \to 0$, i.e. for infinitesimal shear superposed on finite axial stretch, the nonlinear shear modulus, given by (3.3), converges to

$$\widetilde{\mu}(a) = \lim_{\gamma\to 0} \mu(a,\gamma). \tag{3.6}$$

If $a \to 1$ and $\gamma \to 0$, then these shear moduli converge to the linear shear modulus of the infinitesimal theory, i.e.

$$\begin{aligned}
\overline{\mu} &= \lim_{a\to 1}\lim_{\gamma\to 0} \mu(a,\gamma)\\
&= \lim_{\gamma\to 0} \widehat{\mu}(\gamma)\\
&= \lim_{a\to 1} \widetilde{\mu}(a).
\end{aligned} \tag{3.7}$$

Open-cell model. For the open-cell constitutive model (2.21), the nonlinear shear modulus (3.3) is

$$\begin{aligned}
\mu^{(o)}(a,\gamma) = {}& \frac{\mu_w \rho_w^{(o)}(1+k)}{\alpha_1\alpha_2\alpha_3\,(\alpha_1+\alpha_2)}\left[(\alpha_1+\alpha_2)\,(1+k) - k + \frac{k}{[\alpha_1(1+k)-k]\,[\alpha_2(1+k)-k]}\right]\\
&- \frac{\lambda_w \rho_w^{(o)} k(1+k)}{\alpha_1\alpha_2\alpha_3\,(\alpha_1+\alpha_2)}\,\frac{\ln[\alpha_1(1+k)-k] + \ln[\alpha_2(1+k)-k] + \ln[\alpha_3(1+k)-k]}{[\alpha_1(1+k)-k]\,[\alpha_2(1+k)-k]}.
\end{aligned} \tag{3.8}$$

When $a \to 1$, the nonlinear shear modulus given by (3.5) is equal to

$$\widehat{\mu}^{(o)}(\gamma) = \lim_{a\to 1} \mu^{(o)}(a,\gamma), \tag{3.9}$$

and if $\gamma \to 0$, then the nonlinear shear modulus defined by (3.6) is

$$\widetilde{\mu}^{(o)}(a) = \lim_{\gamma\to 0} \mu^{(o)}(a,\gamma). \tag{3.10}$$

In the linear elastic limit [37], $a \to 1$ and $\gamma \to 0$, by (2.1), these shear moduli converge to

$$\begin{aligned}
\overline{\mu}^{(o)} &= \lim_{a\to 1}\lim_{\gamma\to 0} \mu^{(o)}(a,\gamma)\\
&= \mu_w \rho_w^{(o)} (1+k)^2\\
&= \mu_w \frac{3k^2}{1+k}.
\end{aligned} \tag{3.11}$$

Closed-cell model. Similarly, for the closed-cell model (2.24), the nonlinear shear modulus (3.3) is equal to

$$\begin{aligned}
\mu^{(c)}(a,\gamma) = {}& \frac{\mu_w \rho_w^{(c)}(1+k)}{\alpha_1\alpha_2\alpha_3\,(\alpha_1+\alpha_2)}\left[(\alpha_1+\alpha_2)\,(1+k) - k + \frac{k}{[\alpha_1(1+k)-k]\,[\alpha_2(1+k)-k]}\right]\\
&- \frac{\lambda_w \rho_w^{(c)} k(1+k)}{\alpha_1\alpha_2\alpha_3\,(\alpha_1+\alpha_2)}\,\frac{\ln[\alpha_1(1+k)-k] + \ln[\alpha_2(1+k)-k] + \ln[\alpha_3(1+k)-k]}{[\alpha_1(1+k)-k]\,[\alpha_2(1+k)-k]}\\
&+ \frac{\mu_c \rho_c^{(c)}}{\alpha_1\alpha_2\alpha_3}.
\end{aligned} \tag{3.12}$$

When $a \to 1$, the nonlinear shear modulus (3.5) is

$$\widehat{\mu}^{(c)}(\gamma) = \lim_{a\to 1} \mu^{(c)}(a,\gamma), \tag{3.13}$$

and if $\gamma \to 0$, then the nonlinear shear modulus (3.6) is

$$\widetilde{\mu}^{(c)}(a) = \lim_{\gamma\to 0} \mu^{(c)}(a,\gamma). \tag{3.14}$$

In the linear elastic limit [38], $a \to 1$ and $\gamma \to 0$, by (2.2) and (2.3), these moduli converge to

$$\begin{aligned} \overline{\mu}^{(c)} &= \lim_{a\to 1}\lim_{\gamma\to 0} \mu^{(c)}(a,\gamma) \\ &= \mu_w \rho_w^{(c)} (1+k)^2 + \mu_c \rho_c^{(c)} \\ &= 3k\mu_w + \mu_c \frac{1}{(1+k)^3}. \end{aligned} \tag{3.15}$$

When the closed cells are empty, by setting $\rho_c^{(c)} = 0$ in (3.12), (3.13), (3.14), and (3.15), respectively, we obtain the corresponding nonlinear shear moduli, $\mu^{(e)}$, $\widehat{\mu}^{(e)}$, $\widetilde{\mu}^{(e)}$, and $\overline{\mu}^{(e)}$.

4 Stretch modulus and Poisson function

Next, for the mesoscopic models (2.21) and (2.24), we derive explicitly the corresponding nonlinear stretch modulus and Poisson function under large strain, following the formal definition of these nonlinear elastic parameters and their universal relation given in [35]. For the values of these parameters under infinitesimal deformations, see also [37] and [38]. We focus on the simple extension (or contraction) $\mathrm{diag}(\alpha_1, \alpha_2, \alpha_3)$, with $\alpha_3 = a > 1$ ($a < 1$ for contraction) and $\alpha_1 = \alpha_2 = \alpha(a)$ (as in Figure 5 middle), for which the associated Cauchy stress tensor is equal to $\boldsymbol{\sigma} = \mathrm{diag}\,(0, 0, N)$, with $N > 0$ for uniaxial tension ($N < 0$ for uniaxial compression).

Remark 4.1 *We recall that, for a hyperelastic body subject to uniaxial tension (or compression), the deformation is a simple extension (contraction) in the direction of the tensile (compressive) force if and only if the BE inequalities* (3.4) *hold [3, 32]. By [38], if the BE inequalities are valid for the cell wall material, then these inequalities are valid also for the open- and closed-cell models.*

The *nonlinear Poisson's ratio*, defined in terms of the logarithmic (or Hencky, or true) strain, is equal to the following Poisson function [4, 35]

$$\nu(a) = -\frac{\ln \alpha(a)}{\ln a}. \tag{4.1}$$

Then, the *nonlinear stretch modulus* satisfies the following *universal relation* [35],

$$E(a) = \widetilde{\mu}(a) \frac{a^2 - a^{-2\nu(a)}}{(1+\nu(a)) \ln a} \left(1 + \nu(a) + a\nu'(a) \ln a\right), \tag{4.2}$$

where $\widetilde{\mu}(a)$ and $\nu(a)$ are given by (3.6) and (4.1), respectively, and $\nu'(a) = d\nu(a)/da$ is the derivative of $\nu(a)$ with respect to a.

We note that, for the neo-Hookean models (2.20) and (2.23), the nonlinear Poisson's ratio given by (4.1) is not constant under finite axial stretch (see Appendix 7 for a proof). We denote by $\nu_w(a)$ and $E_w(a)$ the nonlinear Poisson function and stretch modulus for the cell wall, respectively, and similarly, by $\nu_c(a)$ and $E_c(a)$ the nonlinear Poisson function and stretch modulus for the cell core, respectively. The corresponding linear elastic limits are as follows:

$$\begin{aligned} \overline{\nu}_w &= \lim_{a\to 1} \nu_w(a) \\ &= \frac{\lambda_w}{2\,(\mu_w + \lambda_w)}, \\ \overline{E}_w &= \lim_{a\to 1} E_w(a) \\ &= 2\mu_w(1 + \overline{\nu}_w), \end{aligned} \tag{4.3}$$

and

$$\begin{aligned}\overline{\nu}_c &= \lim_{a\to 1}\nu_c(a)\\ &= \frac{\lambda_c}{2\,(\mu_c+\lambda_c)},\\ \overline{E}_c &= \lim_{a\to 1}E_c(a)\\ &= 2\mu_c(1+\overline{\nu}_c).\end{aligned} \tag{4.4}$$

Open-cell model. For the open-cell mesoscopic model (2.21) under the deformation $\mathrm{diag}(\alpha_1,\alpha_2,\alpha_3)$, such that $\alpha_3 = a$ and $\alpha_1 = \alpha_2 = \alpha(a)$ in the Cartesian directions $(\mathbf{e}_1,\mathbf{e}_2,\mathbf{e}_3)$, we assume that some of the cell walls are aligned with these Cartesian directions. Then, their deformation is $\mathrm{diag}(\lambda_1,\lambda_2,\lambda_3)$, where $\lambda_3 = a(1+k)-k$, $\lambda_1 = \lambda_2 = \lambda(a) = \lambda_3^{-\nu_w(\lambda_3)} = [a(1+k)-k]^{-\nu_w(a(1+k)-k)}$, and $\alpha(a) = (\lambda(a)+k)/(1+k)$. In this case, the nonlinear Poisson's ratio, defined by (4.1), is equal to

$$\nu^{(o)}(a) = -\frac{\ln\left\{[a(1+k)-k]^{-\nu_w(a(1+k)-k)}+k\right\}-\ln(1+k)}{\ln a}. \tag{4.5}$$

In the linear elastic limit [37], the Poisson function given by (4.5) converges to

$$\begin{aligned}\overline{\nu}^{(o)} &= \lim_{a\to 1}\nu^{(o)}(a)\\ &= \overline{\nu}_w.\end{aligned} \tag{4.6}$$

The corresponding nonlinear stretch modulus satisfies the following relation similar to (4.2),

$$E^{(o)}(a) = \widetilde{\mu}^{(o)}(a)\frac{a^2-a^{-2\nu^{(o)}(a)}}{(1+\nu^{(o)}(a))\ln a}\left(1+\nu^{(o)}(a)+a(\nu^{(o)})'(a)\ln a\right), \tag{4.7}$$

with $\widetilde{\mu}^{(o)}(a)$ given by (3.10). In the linear elastic limit [37], the nonlinear stretch modulus defined by (4.7) converges to

$$\begin{aligned}\overline{E}^{(o)} &= \lim_{a\to 1}E^{(o)}(a)\\ &= \overline{E}_w\rho_w^{(o)}(1+k)^2\\ &= \overline{E}_w\frac{3k^2}{1+k}.\end{aligned} \tag{4.8}$$

Closed-cell model. Similarly, for the closed-cell model (2.24), if the cells are empty or the Poisson's ratios for the cell walls and the cell core are equal, i.e. $\nu_w = \nu_c$, then the Poisson function and stretch modulus are, respectively,

$$\nu^{(c)}(a) = -\frac{\ln\left\{[a(1+k)-k]^{-\nu_w(a(1+k)-k)}+k\right\}-\ln(1+k)}{\ln a} \tag{4.9}$$

and

$$E^{(c)}(a) = \widetilde{\mu}^{(c)}(a)\frac{a^2-a^{-2\nu^{(c)}(a)}}{(1+\nu^{(c)}(a))\ln a}\left(1+\nu^{(c)}(a)+a(\nu^{(c)})'(a)\ln a\right), \tag{4.10}$$

with $\widetilde{\mu}^{(c)}(a)$ given by (3.14). In the linear elastic limit [38],

$$\begin{aligned}\overline{\nu}^{(c)} &= \lim_{a\to 1}\nu^{(c)}(a)\\ &= \overline{\nu}_w\end{aligned} \tag{4.11}$$

and

$$\begin{aligned}\overline{E}^{(c)} &= \lim_{a\to 1}E^{(c)}(a)\\ &= \overline{E}_w\rho_w^{(c)}(1+k)^2+\overline{E}_c\rho_c^{(c)}\\ &= 3k\overline{E}_w+\overline{E}_c\frac{1}{(1+k)^3}.\end{aligned} \tag{4.12}$$

5 Bulk modulus

In addition, volume changes in the isotropic hyperelastic models (2.21) and (2.24) can be quantified by the following *nonlinear bulk modulus* [35], defined under the equitriaxial stretch $\mathrm{diag}(\alpha_1, \alpha_2, \alpha_3)$, with $\alpha_1 = \alpha_2 = \alpha_3 = a > 0$ (see Figure 6),

$$\kappa = \frac{1}{3} \frac{\partial \left(\sigma_1 + \sigma_2 + \sigma_3 \right)}{\partial (J-1)}, \tag{5.1}$$

where $\{\sigma_i\}_{i=1,2,3}$ are the principal Cauchy stresses and $J = \alpha_1 \alpha_2 \alpha_3 = a^3$.

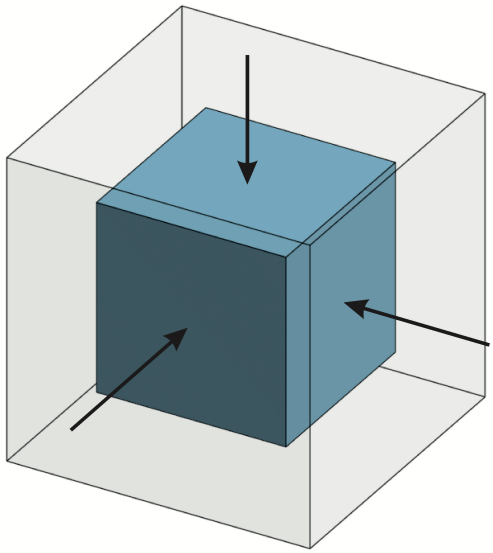

Figure 6: Cube deformed by hydrostatic compression.

Remark 5.1 *For a compressible isotropic material, the fact that the volume of the material is decreased by hydrostatic compression and increased by hydrostatic tension is expressed by the the pressure-compression (PC) inequalities stating that each principal stress is a tension or a compression if the corresponding principal stretch is an extension or a contraction, i.e.* $\sigma_i \left(\alpha_i - 1 \right) > 0$, $i = 1, 2, 3$ *[48, p. 155]. Physically, either or both of the following mean versions of the PC conditions are more realistic,*

$$\sigma_1 \left(\alpha_1 - 1 \right) + \sigma_2 \left(\alpha_2 - 1 \right) + \sigma_3 \left(\alpha_3 - 1 \right) > 0, \tag{5.2}$$

or

$$\sigma_1 \left(1 - \frac{1}{\alpha_1} \right) + \sigma_2 \left(1 - \frac{1}{\alpha_2} \right) + \sigma_3 \left(1 - \frac{1}{\alpha_3} \right) > 0, \tag{5.3}$$

if not all principal stretches are equal to 1. *By [38], if the PC inequalities hold for the cell wall material, then these inequalities hold also for the open- and closed-cell models.*

As J quantifies the relative change of volume from the reference to the current configuration, assuming that J is close to 1 (i.e. for small or incremental volume changes), and setting $\sigma_1 = \sigma_2 = \sigma_3 = \sigma$, the nonlinear bulk modulus (5.1) simplifies as follows,

$$\kappa = \lim_{J \to 1} \frac{\sigma}{J - 1}. \tag{5.4}$$

For the neo-Hookean models (2.20) and (2.23), the respective bulk moduli given by (5.4) are constant and equal to

$$\begin{aligned}\kappa_w &= \frac{2\mu_w + 3\lambda_w}{3},\\ \kappa_c &= \frac{2\mu_c + 3\lambda_c}{3}.\end{aligned} \tag{5.5}$$

Open-cell model. For the open-cell model (2.21), expressing the principal components of the Cauchy stress tensor as

$$\begin{aligned}\sigma_i^{(o)} &= \frac{\mu_w \rho_w^{(o)}(1+k)}{J_o^{2/3}}\left[J_o^{1/3}(1+k) - k - \frac{1}{J_o^{1/3}(1+k)-k}\right]\\ &+ \frac{\lambda_w \rho_w^{(o)}(1+k)}{J_o^{2/3}}\frac{\ln\left[(1+k)^3 J_o - 3k(1+k)^2 J_o^{2/3} + 3k^2(1+k)J_o^{1/3} - k^3\right]}{J_o^{1/3}(1+k)-k}, \qquad i = 1,2,3,\end{aligned} \tag{5.6}$$

where $J_o = a^3$, and the nonlinear bulk modulus given by (5.4) takes on the form

$$\begin{aligned}\kappa^{(o)} &= \lim_{J_o \to 1}\left\{\frac{\mu_w \rho_w^{(o)}(1+k)}{J_o^{2/3}(J_o-1)}\left[J_o^{1/3}(1+k) - k - \frac{1}{J_o^{1/3}(1+k)-k}\right]\right.\\ &\left.+\frac{\lambda_w \rho_w^{(o)}(1+k)}{J_o^{2/3}(J_o-1)}\frac{\ln\left[(1+k)^3 J_o - 3k(1+k)^2 J_o^{2/3} + 3k^2(1+k)J_o^{1/3} - k^3\right]}{J_o^{1/3}(1+k)-k}\right\}\\ &= \kappa_w \rho_w^{(o)}(1+k)^2\\ &= \kappa_w \frac{3k^2}{1+k}.\end{aligned} \tag{5.7}$$

Closed-cell model. Similarly, for the closed-cell model (2.24), the nonlinear bulk modulus defined by (5.4) is equal to

$$\begin{aligned}\kappa^{(c)} &= \lim_{J_c \to 1}\left\{\frac{\mu_w \rho_w^{(c)}(1+k)}{J_c^{2/3}(J_c-1)}\left[J_c^{1/3}(1+k) - k - \frac{1}{J_c^{1/3}(1+k)-k}\right]\right.\\ &+ \frac{\lambda_w \rho_w^{(c)}(1+k)}{J_c^{2/3}(J_c-1)}\frac{\ln\left[(1+k)^3 J_c - 3k(1+k)^2 J_c^{2/3} + 3k^2(1+k)J_c^{1/3} - k^3\right]}{J_c^{1/3}(1+k)-k}\\ &\left.+\frac{\rho_c^{(c)}}{J_c}\left(\mu_c \frac{J_c^{2/3}-1}{J_c-1} + \lambda_c \frac{\ln J_c}{J_c-1}\right)\right\}\\ &= \kappa_w \rho_w^{(c)}(1+k)^2 + \kappa_c \rho_c^{(c)}\\ &= 3k\kappa_w + \kappa_c \frac{1}{(1+k)^3}.\end{aligned} \tag{5.8}$$

Hence, for the open- and the closed-cell models with neo-Hookean cell walls, the nonlinear bulk moduli given by (5.7) and (5.8), respectively, are constant.

6 Examples

For the isotropic hyperelastic models (2.21) and (2.24), we illustrate the nonlinear elastic behaviour under the studied deformations as follows:

- In Figure 7, for the open-cell models, defined by (2.21), with varying thickness to length ratio of the cell wall, $k \in \{0.1, 0.2, 0.3\}$, and fixed cell wall material parameters, $\mu_w = 1$ and $\nu_w = 0.49$, we plot: (A) the nonlinear shear modulus $\widehat{\mu}^{(o)}(\gamma)$, given by (3.9), evaluated under varying simple shear,

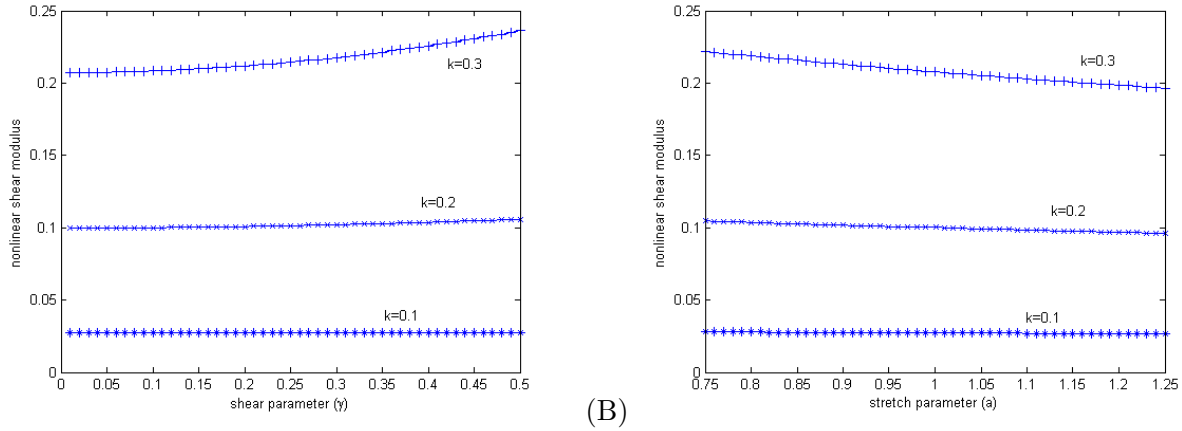

(A) (B)

Figure 7: Open-cell models (2.21) with varying thickness to length ratio of cell wall, $k \in \{0.1, 0.2, 0.3\}$, and fixed $\mu_w = 1$, $\nu_w = 0.49$, showing: (A) nonlinear shear modulus $\widehat{\mu}^{(o)}(\gamma)$ of (3.9), evaluated under varying simple shear ($0 < \gamma < 0.5$) superposed on infinitesimal stretch, and (B) nonlinear shear modulus $\widetilde{\mu}^{(o)}(a)$ of (3.10), evaluated under infinitesimal shear superposed on varying compression or tension ($0.75 < a < 1.25$).

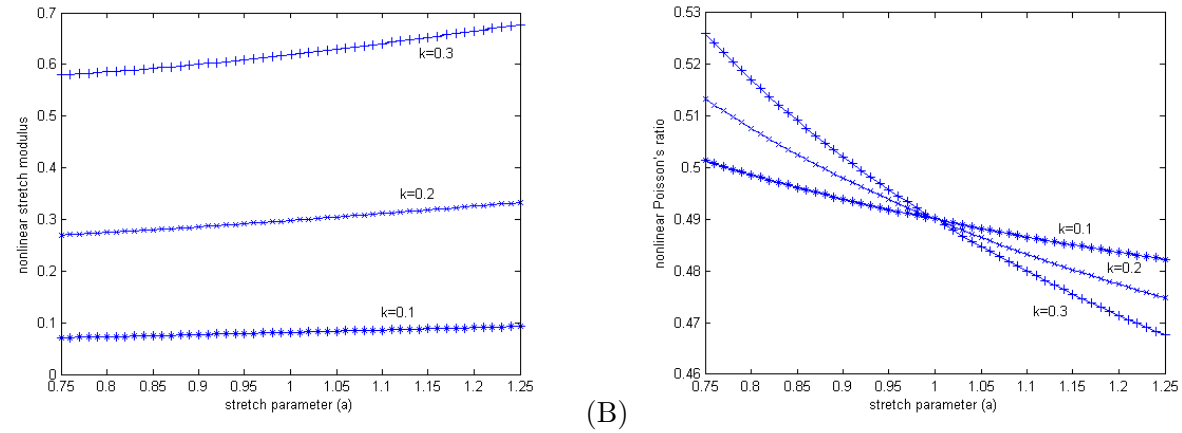

(A) (B)

Figure 8: Open-cell model (2.21) with varying thickness to length ratio of cell wall, $k \in \{0.1, 0.2, 0.3\}$, and fixed $\mu_w = 1$, $\nu_w = 0.49$, showing: (A) nonlinear stretch modulus $E^{(o)}(a)$ of (4.7), and (B) nonlinear Poisson's ratio $\nu^{(o)}(a)$ of (4.5), both evaluated under varying compression or tension ($0.75 < a < 1.25$).

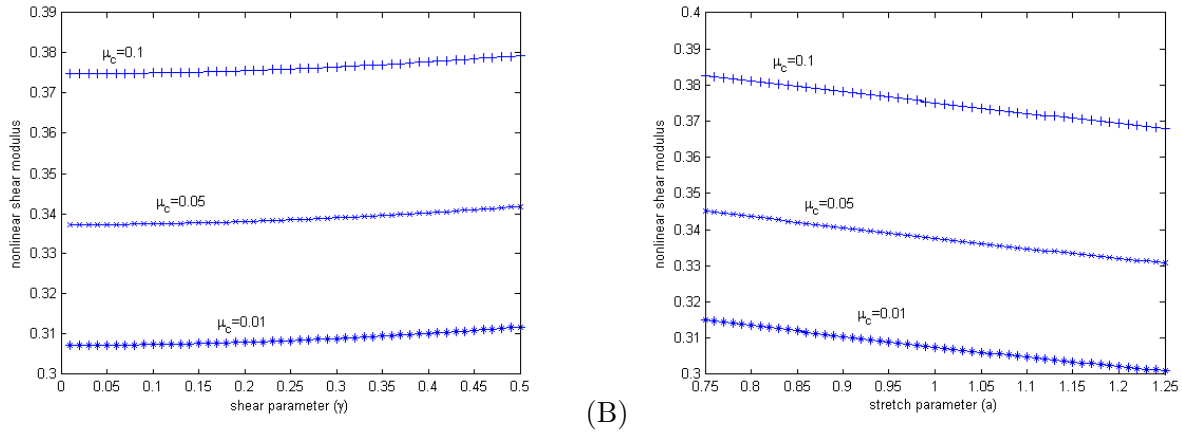

(A) (B)

Figure 9: Closed-cell model (2.24) with varying shear modulus of cell core, $\mu_c \in \{0.01, 0.05, 0.1\}$ and fixed $\mu_w = 1$, $\nu_w = \nu_c = 0.49$, and $k = 0.1$, showing: (A) nonlinear shear modulus $\widehat{\mu}^{(c)}(\gamma)$ of (3.13), evaluated under varying simple shear ($0 < \gamma < 0.5$) superposed on infinitesimal stretch, and (B) nonlinear shear modulus $\widetilde{\mu}^{(c)}(a)$ of (3.14), evaluated under infinitesimal shear superposed on varying compression or tension ($0.75 < a < 1.25$).

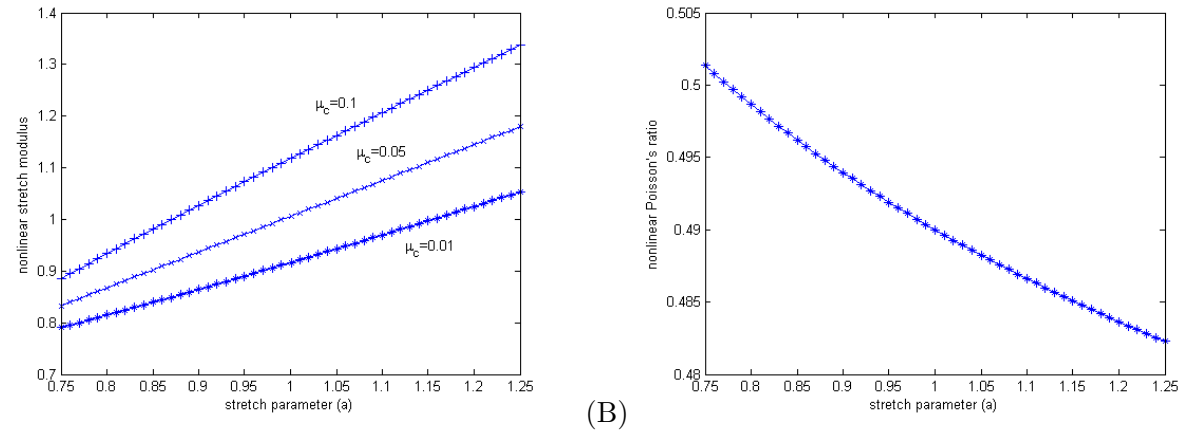

(A) (B)

Figure 10: Closed-cell model (2.24) with varying shear modulus of cell core, $\mu_c \in \{0.01, 0.05, 0.1\}$ and fixed $\mu_w = 1$, $\nu_w = \nu_c = 0.49$, and $k = 0.1$, showing: (A) nonlinear stretch modulus $E^{(c)}(a)$ of (4.10), and (B) nonlinear Poisson's ratio $\nu^{(c)}(a)$ of (4.9), both evaluated under varying compression or tension ($0.75 < a < 1.25$).

with $0 < \gamma < 0.5$, superposed on infinitesimal axial stretch, and (B) the nonlinear shear modulus $\widetilde{\mu}^{(o)}(a)$, given by (3.10), evaluated under infinitesimal shear superposed on varying compression or tension, with $0.75 < a < 1.25$.

- In Figure 8, for the open-cell models (2.21), with varying thickness to length ratio of the cell wall, $k \in \{0.1, 0.2, 0.3\}$, and fixed material parameters, $\mu_w = 1$ and $\nu_w = 0.49$, we show: (A) the nonlinear stretch modulus $E^{(o)}(a)$, given by (4.7), and (B) the nonlinear Poisson's ratio $\nu^{(o)}(a)$, given by (4.5), both evaluated under varying compression or tension, with $0.75 < a < 1.25$.

- In Figure 9, for the closed-cell models, given by (2.24), with varying shear modulus of the cell core, $\mu_c \in \{0.01, 0.05, 0.1\}$, and fixed cell wall parameters, $\mu_w = 1$, $\nu_w = \nu_c = 0.49$, and $k = 0.1$, we plot: (A) the nonlinear shear modulus $\widehat{\mu}^{(c)}(\gamma)$, given by (3.13), evaluated under varying simple shear, with $0 < \gamma < 0.5$, superposed on infinitesimal stretch, and (B) the nonlinear shear modulus $\widetilde{\mu}^{(c)}(a)$, given by (3.14), evaluated under infinitesimal shear superposed on varying compression or tension, with $0.75 < a < 1.25$.

- In Figure 10, for the closed-cell models (2.24), with varying shear modulus of the cell core, $\mu_c \in \{0.01, 0.05, 0.1\}$, and fixed cell wall parameters, $\mu_w = 1$, $\nu_w = \nu_c = 0.49$, and $k = 0.1$, we show: (A) the nonlinear stretch modulus $E^{(c)}(a)$, defined by (4.10), and (B) the nonlinear Poisson's ratio $\nu^{(c)}(a)$, defined by (4.9), both evaluated under varying compression or tension, with $0.75 < a < 1.25$.

7 Discussion

For stretch-dominated cellular structures with open or closed cells made from an arbitrary homogeneous isotropic hyperelastic material, continuum isotropic hyperleastic models at a mesoscopic level were constructed analytically in [37,38]. To gain further insight into the nonlinear elastic behaviour of these models, here, we specialised to the case with neo-Hookean cell components, and derived explicitly the nonlinear shear, stretch, and bulk moduli and Poisson function defined in [35]. Our computed examples show that, for the open-cell model:

- Under simple shear superposed on infinitesimal stretch, the nonlinear shear modulus increases slightly (or remains almost constant) as the shear parameter satisfying $0 < \gamma < 0.5$ increases (Figure 7A).

- Under infinitesimal shear superposed on finite axial stretch, the nonlinear shear modulus decreases (or remains almost) constant as the stretch ratio satisfying $0.75 < a < 1.25$ increases, i.e. the shear modulus increases in compression and decreases in tension (Figure 7B).

- Under increasing finite axial stretch, the nonlinear stretch modulus increases, while the Poisson function decreases (Figure 8).

- As the thickness to length ratio of the cell wall, k, increases, the nonlinear shear and stretch parameters increase, while the nonlinear Poisson's ratio decreases in tension and increases in compression (figures 7 and 8).

Analogous properties were found for the closed-cell model with empty cells (results not shown). In addition, when the closed cells are filled with an elastic core that has the same Poisson's ratio as the cell walls:

- The nonlinear shear and stretch moduli increase as the shear modulus of the cell core, μ_c, increases (figures 9 and 10A).

- When the Poisson's ratios for the cell wall and for the different cell core materials are equal, the nonlinear Poisson's ratio for the closed-cell model does not change with the cell core (Figure 10B).

For the mesoscopic hyperelastic models investigated here, the nonlinear elastic parameters were predicted analytically from the material and geometric parameters at the cell level, which were provided a priori. Conversely, hyperelastic models with specific nonlinear elastic properties may be designed by selecting suitable material and geometric properties of the components.

Similar constitutive models can be derived and analysed computationally for stretch-dominated hierarchical and self-similar structures. These models can be useful in deformation decomposition or multiple scale procedures, where a cellular structure is represented first as a continuum material deforming under finite homogeneous strain. The design of such models and their nonlinear elastic analysis remains to be explored.

Appendix A

In this appendix, we prove that the nonlinear Poisson's ratio defined by (4.1) is not constant for an elastic body characterised by the generalised neo-Hookean model

$$\mathcal{W}(\alpha_1,\alpha_2,\alpha_3)=\frac{\mu}{2}\left[\alpha_1^2+\alpha_2^2+\alpha_3^2-3-\ln(\alpha_1^2\alpha_2^2\alpha_3^2)\right]+\frac{\lambda}{2}\left[\ln(\alpha_1\alpha_2\alpha_3)\right]^2, \tag{7.1}$$

where $\mu>0$ and $\lambda>0$ are constants.

Proof: Under simple tension or compression, $\mathrm{diag}(\alpha_1,\alpha_2,\alpha_3)$, with $\alpha_3=a>0$ and $\alpha_1=\alpha_2=\alpha(a)$, the associated Cauchy stress tensor is equal to $\boldsymbol{\sigma}=\mathrm{diag}\,(0,0,N)$, where $N\neq 0$ and the diagonal components satisfy

$$\sigma_i=J^{-1}\alpha_i\frac{\partial\mathcal{W}}{\partial\alpha_i},\qquad i=1,2,3, \tag{7.2}$$

with $J=\alpha_1\alpha_2\alpha_3$. For the constitutive model (7.1), under the given deformation, (7.2) reduces to

$$\begin{aligned}\frac{1}{\alpha_1^2\alpha_3}\left[\mu(\alpha_1^2-1)+\lambda\ln\left(\alpha_1^2\alpha_3\right)\right]&=0,\\ \frac{1}{\alpha_1^2\alpha_3}\left[\mu(\alpha_3^2-1)+\lambda\ln\left(\alpha_1^2\alpha_3\right)\right]&=N.\end{aligned} \tag{7.3}$$

Equivalently, by subtracting the first from the second equation in (7.3), we obtain

$$\begin{aligned}\mu(\alpha_1^2-1)+\lambda\ln\left(\alpha_1^2\alpha_3\right)&=0,\\ \frac{\mu(\alpha_3^2-\alpha_1^2)}{\alpha_1^2\alpha_3}&=N.\end{aligned} \tag{7.4}$$

Next, using the definition of the Poisson function given by (4.1), if $\alpha_3=a$, then $\alpha_1=\alpha_3^{-\nu(a)}$, and (7.4) takes on the form

$$\begin{aligned}\mu(a^{-2\nu(a)}-1)+\lambda\,(1-2\nu(a))\ln a&=0,\\ \frac{\mu(a^2-a^{-2\nu(a)})}{a^{1-2\nu(a)}}&=N.\end{aligned} \tag{7.5}$$

Assuming constant Poisson function, $\nu(a)=\overline{\nu}=\lambda/(2(\mu+\lambda))$, then $\lambda=2\mu\overline{\nu}/(1-2\overline{\nu})$ and (7.5) reduces to

$$\begin{aligned}a^{-2\overline{\nu}}+2\nu\ln a&=1,\\ \frac{\mu(a^2-a^{-2\overline{\nu}})}{a^{1-2\overline{\nu}}}&=N.\end{aligned} \tag{7.6}$$

Noting that the first equation in (7.6) has the unique solution $a=1$, we conclude that only under infinitesimal strain the Poisson function can be constant, but not under large strains.

References

[1] Adeeb SM, Epstein M. 2009. Fractal elements, Journal of Mechanics of Materials and Structures 4, 781-797.

[2] Ajdari A, Jahromi BH, Papadopoulos J, Nayeb-Hashemi H, Vaziri A. 2012. Hierarchical honeycombs with tailorable properties, International Journal of Solids and Structures 49, 1413-1419.

[3] Baker M, Ericksen JL. 1954. Inequalities restricting the form of stress-deformation relations for isotropic elastic solids and Reiner-Rivlin fluids, Journal of the Washington Academy of Sciences 44, 24-27.

[4] Beatty MF, Stalnaker DO. 1986. The Poisson function of finite elasticity, Journal of Applied Mathematics 53, 807-813.

[5] Beatty MF. 1989. Gent-Thomas and Blatz-Ko models for foamed elastomers. In Mechanics of Cellulosic and Polymeric Materials, AMD v. 99 (MD v. 13), R. W. Perkins ed, American Society of Mechanical Engineering, New York, 75-78.

[6] Beatty MF. 1996. Introduction to nonlinear elasticity. In Nonlinear Effects in Fluids and Solids, M. M. Carroll, M. A. Hayes eds., Plenum Press, New York and London, 13-104.

[7] Beatty MF. 2001. Seven lectures in finite elasticity. In Topics in Finite Elasticity, M. Hayes, G. Saccomandi eds., Springer-Verlag, Wien, 31-93.

[8] Blatz PJ, Ko WL. 1962. Application of finite elastic theory to deformation of rubbery materials, Transactions of The Society of Rheology 6, 223-251.

[9] Broedersz CP, MacKintosh FC. 2014. Modeling semiflexible polymer networks, Review of Modern Physics 86, 995-1036.

[10] Chen H, Zhu F, Jang KI, Feng X, Rogers JA, Zhang Y, Huang Y, Ma Y. 2017. The equivalent medium of cellular substrate under large stretching, with applications to stretchable electronics, Journal of the Mechanics and Physics of Solids, doi: 0.1016/j.jmps.2017.11.002.

[11] Deshpande VS, Ashby MF, Fleck NA. 2001. Foam topology bending versus stretching dominated architectures, Acta Materialia 49, 1035-1040.

[12] Deshpande VS, Fleck NA, Ashby MF. 2001. Effective properties of the octet-truss lattice material, Journal of the Mechanics and Physics of Solids 49, 1747-1769.

[13] Destrade M, Saccomandi G. 2010. On the rectilinear shear of compressible and incompressible elastic slabs, International Journal of Engineering Science 48, 1202-1211.

[14] Discher DE, Janmey P, Wang Y. 2005. Tissue cells feel and respond to the stiffness of their substrate, Science 310, 1139-1143.

[15] Dunlop JWC, Fratzl P. 2013. Multilevel architectures in natural materials, Scripta Materialia 68, 8-12.

[16] Egan P, Ferguson S, Shea K. 2017. Design of hierarchical 3D printed scaffolds considering mechanical and biological factors for bone tissue engineering, Journal of Mechanical Design 139, 061401.

[17] Elsayed MSA, Pasini D. 2010. Multiscale structural design of columns made of regular octet-truss lattice material, International Journal of Solids and Structures 47, 1764-1774.

[18] Engelmayr Jr. GC, Papworth GD, Watkins SC, Mayer Jr. JE, Sacks MS. 2006. Guidance of engineered tissue collagen orientation by large-scale scaffold microstructures, Journal of Biomechanics 39, 1819-1831.

[19] Engler AJ, Sen S, Lee Sweeney H, Discher DE. 2006. Matrix elasticity directs stem cell lineage specification, Cell 126, 677-689.

[20] Epstein M, Adeeb SM. 2008. The stiffness of self-similar fractals, International Journal of Solids and Structures 45, 3238-3254.

[21] Ericksen JL. 1955. Deformation possible in every compressible isotropic perfectly elastic materials, Journal of Mathematics and Physics 34, 126-128.

[22] Fan HL, Jin FN, Fang DN. 2008. Mechanical properties of hierarchical cellular materials. Part I: Analysis, Composites Science and Technology 68, 3380-3387.

[23] Fleck NA, Deshpande VS, Ashby MF. 2010. Micro-architectured materials: past, present and future, Proceedings of the Royal Society of London A: Mathematical, Physical and Engineering Sciences 466, 2495-2516.

[24] Fortes MA, Nogueira MT. 1989. The Poisson effect in cork, Materials Science and Engineering A 122, 227-232.

[25] Gent AN, Thomas AG. 1959. The deformation of foamed elastic materials, Journal of Applied Polymer Science 1, 107-113.

[26] Gent AN, Thomas AG. 1963. Mechanics of foamed elastic materials, Rubber Chemistry and Technology 36, 597-610.

[27] Gibson LJ, Ashby MF. 1997. Cellular Solids: Structure and Properties, 2nd ed, Cambridge University Press, Cambridge, UK.

[28] Gibson LJ, Ashby MF, Harley BA. 2010. Cellular Materials in Nature and Medicine, Cambridge University Press, Cambridge, UK.

[29] Goriely A. 2017. The Mathematics and Mechanics of Biological Growth, Springer, New York.

[30] Hill R. 1978. Aspects of invariance in solid mechanics. Advances in Applied Mechanics 18, 1-75.

[31] Lakes R. 1993. Materials with structural hierarchy, Nature 361, 511-515.

[32] Marzano M. 1983. An interpretation of Baker-Ericksen inequalities in uniaxial deformation and stress, Meccanica 18, 233-235.

[33] Meza LR, Das S, Greer JR. 2014. Strong, lightweight, and recoverable three-dimensional ceramic nanolattices, Science 345, 1322-1326.

[34] Mihai LA, Alayyash K, Goriely A. 2015. Paws, pads, and plants: the enhanced elasticity of cell-filled load-bearing structures, Proceedings of the Royal Society A 471, 20150107.

[35] Mihai LA, Goriely A. 2017. How to characterize a nonlinear elastic material? A review on nonlinear constitutive parameters in isotropic finite elasticity, Proceedings of the Royal Society A 473, 20170607.

[36] Mihai LA, Safar A, Wyatt H. 2018. Debonding of cellular structures with fibre-reinforced cell walls under shear deformation, Journal of Engineering Mathematics 109, 3-19.

[37] Mihai LA, Wyatt H, Goriely A. 2017. A microstructure-based hyperelastic model for open-cell solids, SIAM Journal on Applied Mathematics 77, 1397-1416.

[38] Mihai LA, Wyatt H, Goriely A. 2017. Microstructure-based hyperelastic models for closed-cell solids, Proceedings of the Royal Society A 473, 20170036.

[39] Ogden RW. 1972. Large deformations isotropic elasticity - on the correlation of theory and experiment for incompressible rubberlike solids, Proceedings of the Royal Society A 326, 565-584.

[40] Ogden RW. 1997. Non-Linear Elastic Deformations, 2nd ed, Dover, New York.

[41] Peyton SR, Ghajar CM, Khatiwala CB, Putnam AJ. 2007. The emergence of ECM mechanics and cytoskeletal tension as important regulators of cell function, Cell Biochemistry and Biophysics 47, 300-320.

[42] Rajagopal KR, Wineman AS. 1987. New universal relations for nonlinear isotropic elastic materials, Journal of Elasticity 17, 75-83.

[43] Rayneau-Kirkhope D, Mao Y, Farr R. 2012. Ultralight fractal structures from hollow tubes, Physical Review Letters 109, 204301.

[44] Rumpler M, Woesz A, Dunlop JW, van Dongen JT, Fratzl P. 2008. The effect of geometry on three-dimensional tissue growth, Journal of the Royal Society Interface 5, 1173-1180.

[45] Scanlon MG. 2005. Biogenic cellular solids, in Soft Materials: Structure and Dynamics (Dutcher JR, Marangoni AG eds.), Marcel Dekker, New York, 321-349.

[46] Shield RT. 1971. Deformations possible in every compressible, isotropic, perfectly elastic material, Journal of Elasticity 1, 91-92.

[47] Storakers B. 1986. On the material representation and constitutive branching in finite compressible elasticity, Journal of the Mechanics and Physics of Solids 34, 125-145.

[48] Truesdell C, Noll W. 2004. The Non-Linear Field Theories of Mechanics, 3rd ed, Springer, New York.

[49] Vigliotti A, Pasini D. 2012. Stiffness and strength of tridimensional periodic lattices, Computer Methods in Applied Mechanics and Engineering 229-232, 27-43.

[50] Vigliotti A, Pasini D. 2013. Mechanical properties of hierarchical lattices, Mechanics of Materials 62, 32-43.

[51] Weaire D, Fortes MA. 1994. Stress and strain in liquid and solid foams, Advances in Physics 43, 685-738.

[52] Winer JP, Oake S, Janmey PA. 2009. Non-linear elasticity of extracellular matrices enables contractile cells to communicate local position and orientation, PloS ONE 4, e6382.

[53] Yeung T, Georges PC, Flanagan LA, Marg B, Ortiz M, Funaki M, Zahir N, Ming W, Weaver V, Janmey PA. 2005. Effects of substrate stiffness on cell morphology, cytoskeletal structure, and adhesion, Cell Motility and the Cytoskeleton 60, 2434.

[54] Zhang H, Landmann F, Zahreddine H, Rodriguez D, Koch M, Labouesse M. 2011. A tension-induced mechanotransduction pathway promotes epithelial morphogenesis, Nature 471, 99-103.

[55] Zheng X, Smith W, Jackson JA, Moran B, Cui H, Chen D, Ye J, Fang N, Rodriguez N, Weisgraber TH, Spadaccini CM. 2016. Multiscale metallic metamaterials, Nature Materials 15, 1100-1106.

[56] Zheng X, Lee H, Weisgraber TH, Shusteff M, DeOtte J, Duoss EB, Kuntz JD, Biener MM, Ge Q, Jackson JA, Kucheyev SO, Fang NX, Spadaccini CM. 2014. Ultralight, ultrastiff mechanical metamaterials, Science 344, 1373-1377.